

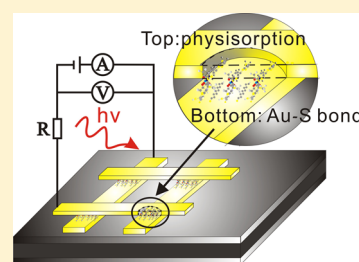
# Conductance Switching and Photovoltaic Effect of Ru(II) Complex Molecular Junctions: Role of Complex Properties and the Metal/Molecule Interface

Jian-Chang Li,\* Jun-Zhi Wu, and Xing Gong

Vacuum and Fluid Engineering Research Center, Northeastern University, Shenyang 110819, People's Republic of China

**ABSTRACT:** The charge transport of Ru(II) complex molecular junctions, fabricated using a soft stamp-printing method, was investigated from 95 to 299 K under both dark and light conditions in order to explore the roles of the electrode/molecule interface and complex properties in the device performance. The junctions show asymmetric current–voltage characteristics with conductance switching and a photovoltaic effect at low temperature. The device performance depends greatly on the redox characteristics and built-in potential induced by electrode/molecule interface(s) and the molecular dipole. Our work may provide valuable information for the design of novel molecular electronics.

**SECTION:** Energy Conversion and Storage; Energy and Charge Transport



Molecular electronics is considered as one of the best solutions to overcome the scaling limits and high cost of conventional semiconductor technology. Currently, an essential task is to understand and control the charge transport through molecules sandwiched between metal contacts. So far, numerous molecules have been reported based on testbeds of metal/molecule/metal junctions for their novel behaviors, such as rectification,<sup>1,2</sup> voltage-driven switching,<sup>3</sup> negative differential resistance (NDR),<sup>4,5</sup> and so forth. Among various organics, ruthenium (Ru) complex molecules attract special attention for their promising photovoltaic,<sup>6</sup> light-emitting diode,<sup>7</sup> and organic bistable memory applications.<sup>8–10</sup> Particularly, there has been increased interest in studying conjugated molecular wires containing a Ru complex component in order to modulate the electronic band structure and to facilitate the charge transport. For example, the introduction of a Ru component into molecular backbones significantly enhanced the conductance, owing to a lower electronic decay constant<sup>11,12</sup> and less band gap<sup>13,14</sup> between the highest occupied molecular orbital (HOMO) and the lowest unoccupied molecular orbital (LUMO). Depending on the relative alignment of molecular orbitals and the Fermi level of the metal electrodes, the redox-active Ru(II) molecules may show functions such as NDR,<sup>15</sup> switching,<sup>16</sup> and rectification.<sup>5,17</sup> Despite these intriguing advances, differentiating the intrinsic electrical properties of the Ru(II) complex from complicated effects due to device structures remains a big challenge.

Especially, to deeply understand the charge transport of Ru(II)-complex-incorporated molecular devices, influences of temperature and light illumination need to be addressed. Using conducting probe atomic force microscopy, Frisibe<sup>18</sup> et al. conducted temperature-dependent measurements and demonstrated that the direct tunneling and thermally activated hopping dominate the charge transport of Ru(II)-incorporated

redox molecules. Meng et al. reported the photo-<sup>19</sup> and electro-<sup>20</sup> triggered reversible conductivity switching of a single Ru-based organometallic molecular junction, which can be promisingly applied as a resettable electronic logic gate. They suggested that by introducing the external orthogonal light irradiation and electrochemical stimuli, the modulated electronic structure between the open and closed isomer states leads to conductivity switching. However, simultaneous temperature- and light-dependent measurements are rarely taken into account. In this Letter, we studied the charge transport of molecular monolayer junctions of a Ru(II)-incorporated oligothiophene with a bipyridine ligand (OTP–Ru) as a function of both temperature and light illumination. Observations of rectification, conductance switching, and photovoltaics were discussed from the effects of the electronic properties of the Ru(II) complex and metal/molecule interface(s).

The chemical structure of the neutral complex OTP–Ru is shown in Figure 1a, which is expected to possess a large dipole moment due to the bipyridine and hexafluoroacetylacetonate bidentate ligand.<sup>5,17</sup> The synthesis is according to the procedure reported previously by Yu et al.<sup>21</sup> The junctions were prepared using a soft print method, as reported previously.<sup>22–24</sup> The junctions were electronically stable up to 300 K for 60 h. Typical current–voltage (*I*–*V*) curves in dark are presented in Figure 1b, showing asymmetric behavior in the entire temperature range. Note that the device initially exhibits an open-circuit behavior with little leakage current from –1.7 to 0.7 V. When the bias sweeps to a particular threshold point, the current increases significantly and then switches to a new conductance state. Compared with that of the oligothiophene

**Received:** January 25, 2014

**Accepted:** March 5, 2014

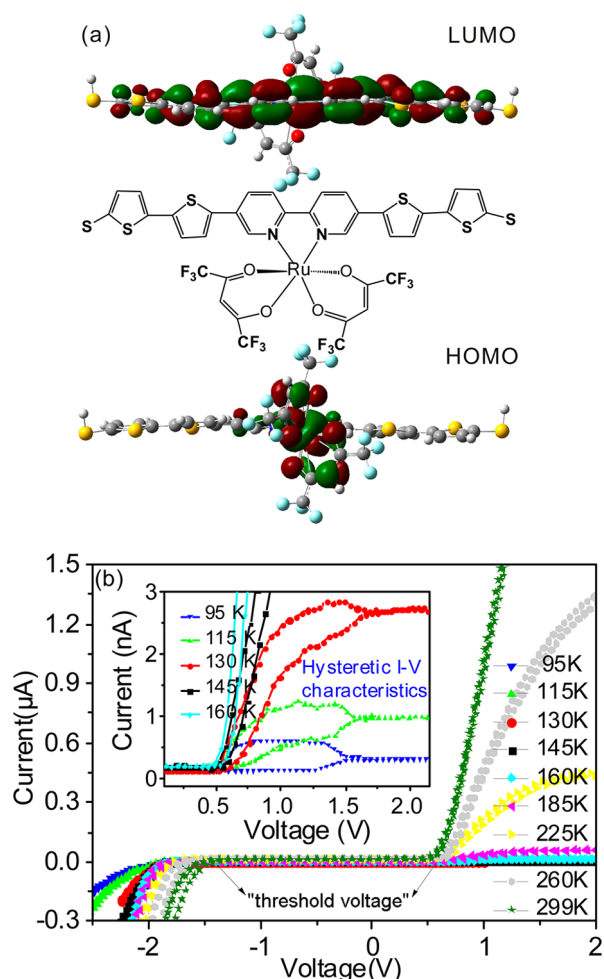


**Figure 1.** (a) Chemical structure of the OTP-Ru molecule and topologies of the HOMO and LUMO. (b) Temperature-dependent  $I$ - $V$  characteristics. (Inset) The hysteresis below 160 K.

derivative that we studied previously,<sup>23</sup> the junction conductivity increases by 2 orders of magnitude. This may be mainly due to the electronic structure modulation of the oligothiophene with the incorporation of a Ru(II) complex.<sup>11</sup>

To explore the modulation effect of a Ru(II) complex, calculations were performed on single oligothiophene and OTP-Ru molecules using the density functional theory method of B3LYP with the 6-31G(d) basis set. As shown in Figure 1a, the LUMO spans the entire oligothiophene with a value of  $-2.9$  eV, whereas the HOMO is located in the Ru fragment and part of the bipyridyl segment with a value of  $-5.3$  eV. The work function of the Au electrode is  $-4.8$  eV. Though the Au Fermi level may deviate a little after contacting with the OTP-Ru wire, the junction charge transport should be a metal-centered HOMO-mediated process (i.e., hole tunneling) because the LUMO is far from the metal Fermi levels. Compared with the 3.1 eV band gap of the oligothiophene, the band gap reduction of 0.7 eV after incorporating the Ru(II) component is expected to increase the conductance<sup>25,26</sup> and further to facilitate the light or thermally excited charge transport through the molecules.<sup>7</sup>

Remarkable temperature and bias polarity dependences are observed in the dark. The device conductivity decreases monotonically as the temperature drops. For example, the current at +1 V decreases by about 4 orders of magnitude as the

temperature decreases from 299 to 95 K. The derived rectification ratio  $[I(+1.0 \text{ V})/I(-1.0 \text{ V})]$ , different from our previous observation for oligothiophene derivatives without a Ru(II) component,<sup>23,24</sup> remains high up to 2 orders of magnitude even at high temperature or under light illumination. This can be owed to the contribution of the permanent dipole moment of the OTP-Ru molecule,<sup>17</sup> which is calculated to be 8.31 D along the direction from acetoacetate to the bipyridine ligand. Indeed, the role of the molecular dipolar orientation in the current rectification has been demonstrated in the monocobalt(II) and dicobalt(II) complexes with the same ligands. The pronounced rectifying effect becomes weaker when the dipole moment is canceled by placing the oppositely located cobalt ion.<sup>5</sup>

Interestingly, the  $I$ - $V$  plots present hysteresis with conductance switching at a positive bias region below 160 K (see the inset of Figure 1b). When the bias is scanned from 0 to +3 V, the junctions switch to a high conductance state after about 0.5 V. Then, they drop to low conductance at about 1.25 V in the reverse scan. However, no such hysteretic behavior was observed in our previous studies of decanethiol and oligo(3-methylthiophene).<sup>23</sup> We thus suggest that this memory effect may result from the charge-accepting nature of the Ru(II) redox-active complex,<sup>9</sup> that is, the charge transfer and storage in the discrete redox state via oxidation and reduction reactions.<sup>10,25</sup> In detail, the electron first tunnels out from the bottom electrode into the ligand-centered LUMO (electron reduction), maintaining an OFF state. The electron then tunnels out from the ligand of the OTP-Ru into the top electrode (electron oxidation), maintaining an ON state. Note that the hysteresis disappears above 145 K, which can be explained by the intensified intermolecular interaction. As reported in our previous study, the conformational changes and the thermionic conductance among neighboring molecules in the crossbar junctions are weak and can be neglected at low temperature,<sup>26</sup> while the intermolecular interactions become enhanced at higher temperature, which further overwhelms the unique single-molecular electronic characteristics.<sup>24,27</sup>

Under light illumination, the  $I$ - $V$  characteristics show little temperature dependence (Figure 2a), while remarkable temperature-dependent optoelectronic switching is observed. As summarized in the inset, the current ratio between the light and dark states at +0.85 V drops drastically from about  $10^4$  to 2.6 as the temperature increase from 95 to 299 K. As reported by Huang et al., this decreased optoelectronic switching can be explained by the functional similarity of temperature and light illumination.<sup>7</sup> The reversible room-temperature photoresponse of OTP-Ru may have promising applications in photosensitive resistors and diodes. Open-circuit behavior is also observed with little leakage current from  $-1.5$  to 0.3 V, while the threshold voltage for a sudden increasing current increases as the temperature rises. Similar experimental<sup>28</sup> and theoretical<sup>29</sup> observations have been reported for stronger electrode/molecule coupling. The slight negative temperature dependence of the rectification ratio from 0.5 to 1.0 V (see Figure 2b) also indicates enhanced coupling between the physisorbed top electrode and the OTP-Ru self-assembled monolayers (SAMs) under light illumination.

Moreover, the OTP-Ru junction displays interesting photovoltaic properties below 225 K (see Figure 2c). The open-circuit voltage  $V_{oc}$  and the short-circuit current  $J_{sc}$  at 185 K were calculated to be 1.78 mV/cm<sup>2</sup> and  $-1.7$  V, respectively. Such behavior may be favorable for applications in novel solar

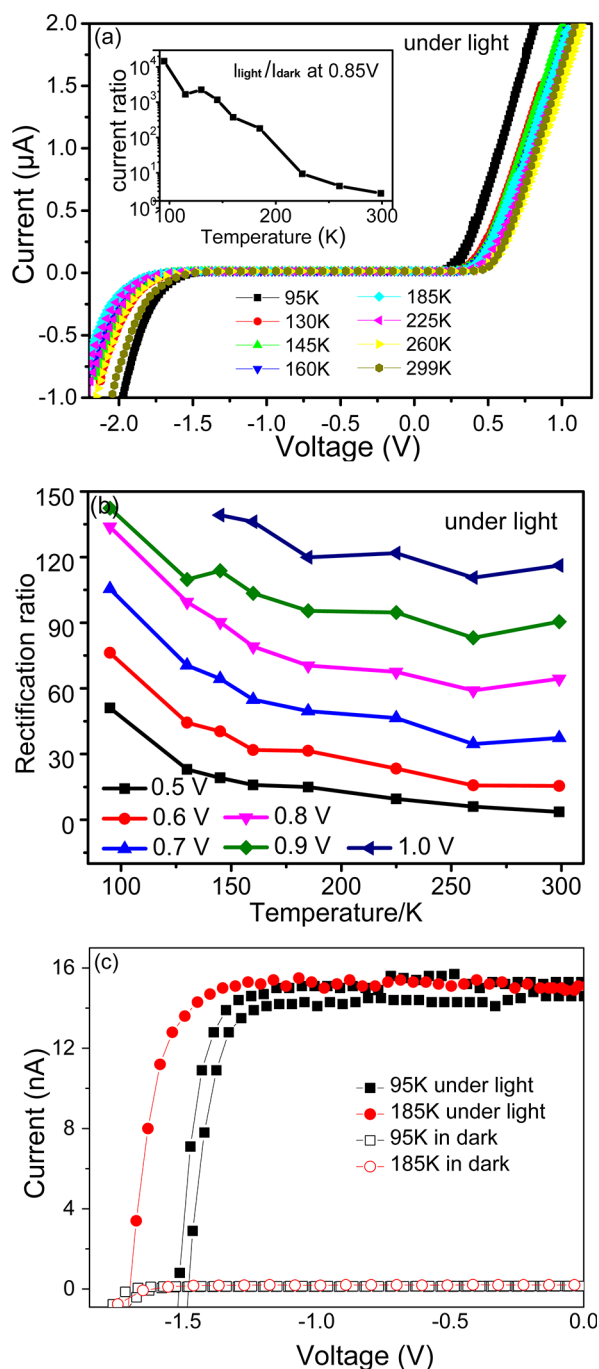


**Figure 2.** (a) Temperature-independent  $I$ - $V$  curves of the Au/OTP-Ru/Au junction under light illumination. (Inset) The current ratio between the light and dark states at +0.85 V from 95 to 299 K. (b) Calculated rectification ratio of the OTP-Ru junction at different biases from 95 to 185 K under light. (c) Photovoltaic effect at low temperature.

cells. To explain the above observations, schematic energy diagrams are depicted in Figure 3. When the OTP-Ru molecules are self-assembled into the insulator spacer matrix of a 1-decanethiol monolayer grown on the bottom Au electrode, they tilt due to the S-Au bond. The alignment of the vacuum level  $E_{\text{vac}}$  and the Fermi level  $E_{\text{F}}$  at surface of the electrodes will become uneven due to the interfacial dipole layer formed by the projected component dipole moment along the direction toward the electrode and the interface difference resulting from

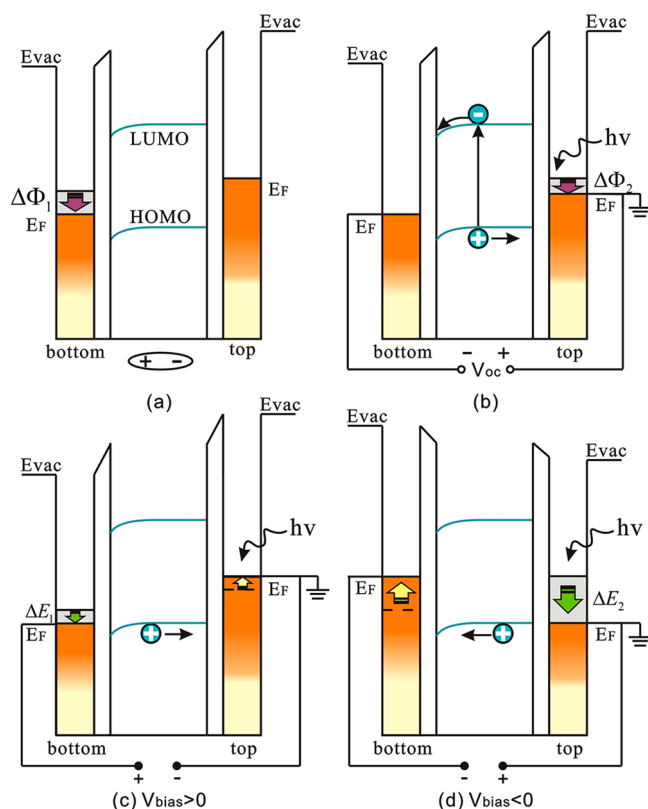


**Figure 3.** Schematic energy diagrams for the charge transport through the Au/OTP-Ru/Au junction at (a) equilibrium in the dark, (b) equilibrium under light, (c) positive bias under light, and (d) negative bias under light.  $E_{\text{vac}}$ : vacuum level at the surface;  $E_{\text{F}}$ : the Fermi level of the electrode;  $V_{\text{oc}}$ : the open-circuit voltage;  $\Delta\Phi_1$ : the  $E_{\text{F}}$  difference due to the different adsorption nature;  $\Delta\Phi_2$ : the decrease of the  $E_{\text{F}}$  difference under light or high temperature;  $\Delta E_1$  and  $\Delta E_2$ : enough positive and negative applied bias to enable the  $E_{\text{F}}$  to align with the HOMO.

the different adsorption nature<sup>30,31</sup> (indicated as  $\Delta\Phi_1$  in Figure 3a). The  $E_{\text{F}}$  difference between the bottom and top electrodes can result in a built-in electrical field. Under light, a great number of excitons may generate due to the low band gap of the OTP-Ru wire. In turn, the built-in potential drives the charge carriers and leads to a photovoltaic effect (see Figure 3b).

When a negative or positive bias is applied to the device, the  $E_{\text{F}}$  of the electrode at one side would shift the HOMO downward to allow charge injection. As indicated by  $\Delta E_1$  in Figure 3c, a relatively small positive bias can bring the  $E_{\text{F}}$  of the bottom electrode to align with the HOMO. On the other hand, the difference between the  $E_{\text{F}}$  of the top electrode and the HOMO is obviously larger (indicated as by  $\Delta E_2$  in Figure 3d). This fact explains the rectification behaviors well. Moreover, owing to the significant strengthened top physisorbed SAMs/Au contact upon light illumination or at high temperature, the  $E_{\text{F}}$  of the top electrode shifts downward and lessens the difference between the two electrodes (signed as  $\Delta\Phi_2$  in Figure 3b). The combination effects of the decreased Fermi level difference and molecular dipole result in the slight negative temperature dependence of the rectification, despite a higher rectification ratio in the dark.

In summary, we demonstrate the role of the Ru(II) complex and SAMs/electrode interface in the junction charge transport by conducting simultaneous temperature- and light-dependent



$I$ – $V$  measurements. The conductivity switching at low temperature in the dark may result from a charging/discharging process in the redox center of the OTP–Ru complex, while the predominant rectification effect under high temperature or light illumination is attributed to the interfacial dipole induced by both the molecular dipole and molecule/electrode contacts. The built-in electrical field aroused from different Fermi levels of the electrodes gives rise to the photovoltaic effect. Our work may provide some clues for developing novel molecular devices based on the Ru(II) complex.

## EXPERIMENTAL METHODS

The addressable OTP–Ru crossbar junctions were fabricated using a polymer stamp-printing method. Briefly, bottom Au electrodes were first fabricated by a standard photolithography technique on a Si substrate with 200 nm thermal oxides on both sides. A sequential deprotection and self-assembly processes were followed in a 1 mM tetrahydrofuran solution of OTP–Ru and decanethiol with a molar ratio of 1:1 for 24 h. Finally, the top Au electrodes precoated on a poly-(dimethylsiloxane) stamp were transferred onto the self-assembled monolayers (SAMs) to form the junctions. The sample was then loaded into a vacuum chamber where low-frequency (0.002 Hz) AC  $I$ – $V$  characteristics were measured using a HP 3325A synthesizer/function generator and a Keithley 619 electrometer from 95 to 295 K with/without light illumination.

## AUTHOR INFORMATION

### Corresponding Author

\*E-mail: jcli@mail.neu.edu.cn.

### Notes

The authors declare no competing financial interest.

## ACKNOWLEDGMENTS

Financial support comes from the Fundamental Research Funds for Central Universities of China (N110403001 and N130403001).

## REFERENCES

- (1) Batra, A.; Darancet, P.; Chen, Q.; Meisner, J. S.; Widawsky, J. R.; Neaton, J. B.; Nuckolls, C.; Venkataraman, L. Tuning Rectification in Single-Molecular Diodes. *Nano Lett.* **2013**, *13*, 6233–6237.
- (2) Nijhuis, C. A.; Reus, W. F.; Whitesides, G. M. Mechanism of Rectification in Tunneling Junctions Based on Molecules with Asymmetric Potential Drops. *J. Am. Chem. Soc.* **2010**, *132*, 18386–18401.
- (3) Tsoi, S.; Griva, I.; Trammell, S. A.; Blum, A. S.; Schnur, J. M.; Lebedev, N. Electrochemically Controlled Conductance Switching in a Single Molecule: Quinone-Modified Oligo(phenylene vinylene). *ACS Nano* **2008**, *2*, 1289–1295.
- (4) Kabehie, S.; Stieg, A. Z.; Xue, M.; Liong, M.; Wang, K. L.; Zink, J. I. Surface Immobilized Heteroleptic Copper Compounds As State Variables That Show Negative Differential Resistance. *J. Phys. Chem. Lett.* **2010**, *1*, 589–593.
- (5) Lee, Y. G.; Yuan, S. W.; Yu, L. P. Dipolar and Electronic Effects on Charge Transport through Single Transition Metal Complexes. *Sci. China Chem.* **2011**, *54*, 410–414.
- (6) Hussain, M.; El-Shafei, A.; Islam, A.; Han, L. Y. Structure–Property Relationship of Extended  $\pi$ -Conjugation of Ancillary Ligands with and without an Electron Donor of Heteroleptic Ru(II) Bipyridyl Complexes for High Efficiency Dye-Sensitized Solar Cells. *Phys. Chem. Chem. Phys.* **2013**, *15*, 8401–8408.
- (7) Huang, W.; Tanaka, H.; Ogawa, T. Effects of Metal–Ion Complexation for the Self-Assembled Nanocomposite Films Composed of Gold Nanoparticles and 3,8-Bis(terthiophenyl)-phenanthroline-Based Dithiols Bridging 1  $\mu$ m Gap Gold Electrodes: Morphology, Temperature Dependent Electronic Conduction, and Photoresponse. *J. Phys. Chem. C* **2008**, *112*, 11513–11526.
- (8) Seo, K.; Konchenko, A. V.; Lee, J.; Bang, G. S.; Lee, H. Molecular Conductance Switch-On of Single Ruthenium Complex Molecules. *J. Am. Chem. Soc.* **2008**, *130*, 2553–2559.
- (9) Pradhan, B.; Das, S. Role of New Bis(2,2'-bipyridyl)-(triazolopyridyl)ruthenium(II) Complex in the Organic Bistable Memory Application. *Chem. Mater.* **2008**, *20*, 1209–1211.
- (10) Lee, J.; Chang, H.; Kim, S.; Bang, G. S.; Lee, H. Molecular Monolayer Nonvolatile Memory with Tunable Molecules. *Angew. Chem., Int. Ed.* **2009**, *48*, 8501–8504.
- (11) Liu, K.; Wang, X. H.; Wang, F. S. Probing Charge Transport of Ruthenium-Complex- Based Molecular Wires at the Single-Molecule Level. *ACS Nano* **2008**, *2*, 2315–2323.
- (12) Kim, B. S.; Beebe, J. M.; Olivier, C.; Rigaut, S.; Touchard, D.; Kushmerick, J. G.; Zhu, X. Y.; Frisbie, C. D. Temperature and Length Dependence of Charge Transport in Redox-Active Molecular Wires Incorporating Ruthenium(II) Bis( $\sigma$ -arylacetylide) Complexes. *J. Phys. Chem. C* **2007**, *111*, 7521–7526.
- (13) Blum, A. S.; Parish, D. A.; Trammell, S. A.; Moore, M. H.; Kushmerick, J. G.; Xu, G. L.; Deschamps, J. R.; Pollack, S. K.; Shashidhar, R. Ru<sub>2</sub>(ap)<sub>4</sub>( $\sigma$ -oligo(phenyleneethynyl)) Molecular Wires: Synthesis and Electronic Characterization. *J. Am. Chem. Soc.* **2005**, *127*, 10010–10011.
- (14) Huang, W.; Masuda, G.; Maeda, S.; Tanakat, H.; Hino, T.; Ogawa, T. Syntheses, Crystal Structures, and Spectral Properties of a Series of 3,8-Bisphenyl-1,10-phenanthroline Derivatives: Precursors of 3,8-Bis(4-mercaptophenyl)-1,10-phenanthroline and Its Ruthenium(II) Complex for Preparing Nanocomposite Junctions with Gold Nanoparticles between 1  $\mu$ m Gap Gold Electrodes. *Inorg. Chem.* **2008**, *47*, 468–480.
- (15) Ng, Z. Y.; Loh, K. P.; Li, L. Q.; Ho, P.; Bai, P.; Yip, J. H. K. Synthesis and Electrical Characterization of Oligo(phenylene ethynylene) Molecular Wires Coordinated to Transition Metal Complexes. *ACS Nano* **2009**, *3*, 2103–2114.
- (16) Seo, S.; Lee, J.; Choi, S. Y.; Lee, H. Multilevel Conductance Switching for a Monolayer of Redox-Active Metal Complexes through Various Metallic Contacts. *J. Mater. Chem.* **2012**, *22*, 1868–1875.
- (17) Lee, Y.; Yuan, S. W.; Sanchez, A.; Yu, L. P. Charge Transport Mediated by D-Orbitals in Transition Metal Complexes. *Chem. Commun.* **2008**, *54*, 247–249.
- (18) Luo, L.; Benameur, A.; Brignou, P.; Choi, S. H.; Rigaut, S.; Frisbie, C. D. Length and Temperature Dependent Conduction of Ruthenium-Containing Redox-Active Molecular Wires. *J. Phys. Chem. C* **2011**, *115*, 19955–19961.
- (19) Meng, F.; Hervault, Y. M.; Norel, L.; Costuas, K.; Dyck, C. V.; Geskin, V.; Cornil, J.; Hng, H. H.; Rigaut, S.; Chen, X. D. Photo-Modulable Molecular Transport Junctions Based on Organometallic Molecular Wires. *Chem. Sci.* **2012**, *3*, 3113–3118.
- (20) Meng, F.; Hervault, Y. M.; Shao, Q.; Hu, B.; Norel, L.; Rigaut, S.; Chen, X. Orthogonally Modulated Molecular Transport Junctions for Resettable Electronic Logic Gates. *Nat. Commun.* **2014**, DOI: 10.1038/ncomms4023.
- (21) Wang, Q.; Yu, L. P. Conjugated Polymers Containing Mixed-Ligand Ruthenium(II) Complexes. Synthesis, Characterization, and Investigation of Photoconductive Properties. *J. Am. Chem. Soc.* **2000**, *122*, 11806–11811.
- (22) Li, J. C. Optoelectronic Switching of Addressable Self-Assembled Monolayer Molecular Junctions. *Chem. Phys. Lett.* **2009**, *473*, 189–192.
- (23) Li, J. C.; Wang, D.; Ba, D. C. Effects of Temperature and Light Illumination on the Current–Voltage Characteristics of Molecular Self-Assembled Monolayer Junctions. *J. Phys. Chem. C* **2012**, *116*, 10986–10994.

- (24) Li, J. C.; Gong, X. Diode Rectification and Negative Differential Resistance of Dipyrimidinyl–Diphenyl Molecular Junctions. *Org. Electron.* **2013**, *14*, 2451–2458.
- (25) Seo, K.; Konchenko, A. V.; Lee, J.; Bang, G. S.; Lee, H. Electron Transport Processes in On/Off States of a Single Alkyl-Tailed Metal Complex Molecular Switch. *J. Mater. Chem.* **2009**, *19*, 7617–7624.
- (26) Schull, T. L.; Kushmerick, J. G.; Patterson, C. H.; George, C.; Moore, M. H.; Pollack, S. K.; Shashidhar, R. Ligand Effects on Charge Transport in Platinum(II) Acetylides. *J. Am. Chem. Soc.* **2003**, *125*, 3202–3203.
- (27) Li, J. C.; Wu, J. Z.; Gong, X.; Zhou, C. Electron Transport of Oligothiophene Derivative Molecular Device at Varied Temperature and Light Illumination. *Org. Electron.* **2014**, DOI: 10.1016/j.orgel.2014.02.012.
- (28) Li, C.; Fan, W.; Straus, D. A.; Lei, B.; Asano, S.; Zhang, D. H.; Han, J.; Meyyappan, M.; Zhou, C. W. Charge Storage Behavior of Nanowire Transistors Functionalized with Bis(terpyridine)-Fe(II) Molecules: Dependence on Molecular Structure. *J. Am. Chem. Soc.* **2004**, *126*, 7750–7751.
- (29) Dhungana, K. B.; Mandal, S.; Pati, R. Switching of Conductance in a Molecular Wire: Role of Junction Geometry, Interfacial Distance, and Conformational Change. *J. Phys. Chem. C* **2012**, *116*, 17268–17273.
- (30) Ishii, H.; Sugiyama, K.; Ito, E.; Seki, K. Energy Level Alignment and Interfacial Electronic Structures at Organic/Metal and Organic/Organic Interfaces. *Adv. Mater.* **1999**, *11*, 605–625.
- (31) Crispin, X. Interface Dipole at Organic/Metal Interfaces and Organic Solar Cells. *Sol Energy Mater. Sol Cells* **2004**, *83*, 147–168.